Electronic Supplementary Information

Second Near-Infrared Photoactivatable Biocompatible Polymer Nanoparticles for Effective in Vitro and in Vivo Cancer Theranostics

Fei Wang,‡[a] Xiaoju Men,‡[b] Haobin Chen,[c] Feixue Mi,[c] Mengze Xu,[b] Xiaoxiao Men,[c] Zhen Yuan,*[b] and Pik Kwan Lo*[a,d]

[a] Department of Chemistry, City University of Hong Kong, Tat Chee Avenue, Kowloon Tong, Hong Kong SAR, China

[b] Faculty of Health Sciences, Center for Cognitive and Brain Sciences, University of Macau, Macau SAR 999078, China

[c] Department of Biomedical Engineering, Southern University of Science and Technology, Shenzhen, Guangdong 518055, China

[d] Key Laboratory of Biochip Technology, Biotech and Health Care, Shenzhen Research Institute of City University of Hong Kong, Shenzhen, Guangdong 518057, China

‡ These authors contributed equally.

*Corresponding Author:

Pik Kwan Lo, Email: peggylo@cityu.edu.hk;

Zhen Yuan, Email: zhenyuan@um.edu.mo.

1. Materials and Experimental Section

1.1 Materials

Tetrakis(triphenylphosphine) palladium(0) (Pd[PPh$_3$]$_4$, 99%), chloroform-d, and (4,4,5,5-tetramethyl-1,3,2-dioxaborolan-2-yl)benzene were purchased from J&K Chemical Ltd., China. Tetra-n-butylammonium bromide (TBAB) was purchased from Aladdin Chemistry Co. Ltd., China. 2,6-bis(trimethyltin)-4,8-bis(5-(2-ethylhexyl)thiophen-2-yl)benzo[1,2-b:4,5-b']dithiophene and 4,8-dibromo-6-(2-ethylhexyl)-[1,2,5]thiadiazolo[3,4-f]benzotriazole were purchased from Derthon Optoelectronic Materials Science & Technology Co., Ltd., China.

1.2 Synthesis of Conjugated Polymer BDT-TBZ

The conjugated polymer poly([4,8-bis(5-(2-ethylhexyl)thiophen-2-yl)benzo[1,2-b:4,5-b']dithiophene-2,6-diyl]-co-[6-(2-ethylhexyl)-[1,2,5]thiadiazolo[3,4-f]benzotriazole-4,8-diyl]) (BDT-TBZ) was synthesized through a combination of donor-acceptor moieties by Stille cross-coupling polymerization as shown in Figure S1. In a 25-mL three-necked flask, the monomer 4,8-dibromo-6-(2-ethylhexyl)-[1,2,5]thiadiazolo[3,4-f]benzotriazole (112 mg, 0.25 mmol) was dissolved in toluene (10 mL) with 2,6-bis(trimethyltin)-4,8-bis(5-(2-ethylhexyl)thiophen-2-yl)benzo[1,2-b:4,5-b']dithiophene (226 mg, 0.25 mmol). The reactant mixtures were stirred at room temperature, and then the flask was degassed and recharged with nitrogen (repeated 3 times) to remove air before and after adding the catalyst Pd(PPh$_3$)$_4$ (5 mg, 0.004 mmol). The mixed solutions were stirred at 100°C for 1 days under a nitrogen atmosphere, and then 1 mL of (4,4,5,5-tetramethyl-1,3,2-dioxaborolan-2-yl)benzene (20 mg, dissolved in toluene) and 0.2 mL of bromobenzene were gradually added dropwise to reactants to remove the end groups separately. Once the hot solution reached ambient temperature, the solution was washed with ultrapure water and purified through Soxhlet extraction, after which it was recrystallized (methanol) and evaporated (vacuum). Product: black-green solid; yield: 166 mg; η: 72%.

^{1}H NMR spectra were recorded using a Varian Mercury 300 MHz spectrometer. Chemical shifts were reported in ppm (δ) relative to tetramethylsilane (TMS, δ = 0.00

ppm) as the internal standard. ^{1}H NMR (300 MHz, CDCl$_3$, δ): 7.85–6.75 (br, 6H), 4.92–4.47 (br, 2H), 3.46–2.72 (br, 4H), 2.65–2.53 (br, 1H), 2.16–0.51 (br, 44H).

The molecular weight and polydispersity of the prepared polymers were measured by Gel Permeation Chromatography as Mn = 472823, Mw = 483681, PDI = 1.02, Mz/Mw = 1.02 (Figure S2) (GPC, 515HPLC pump, Waters, 2414 refractive index detector) in trichloromethane using a calibration curve of polystyrene standards.
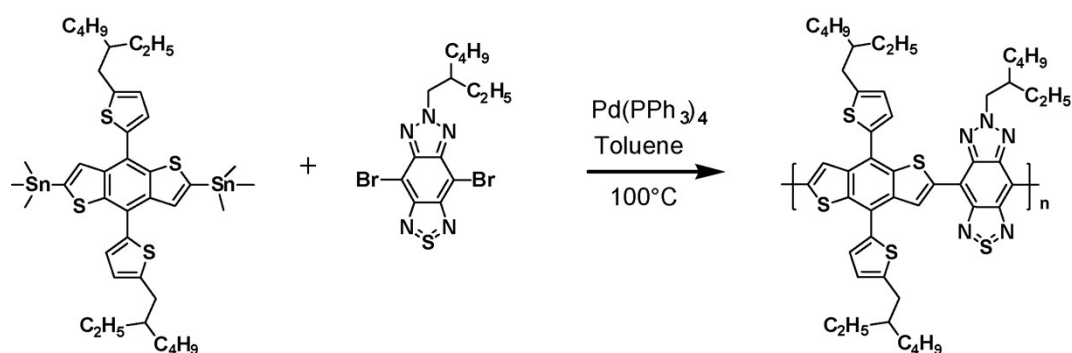
2. Supplementary Figures

Figure S1. Schematic illustration of the synthetic routes of conjugated polymer BDT-TBZ.

GPC Results

	Dist Name	Elution Volume (ml)	Retention Time (min)	Adjusted RT (min)	Mn	Mw	MP	Mz	Mz+1	Mz/Mw	Mz+1/Mw
1		9.940	9.940	9.940	472823	483681		493935	503420	1.021199	1.040809

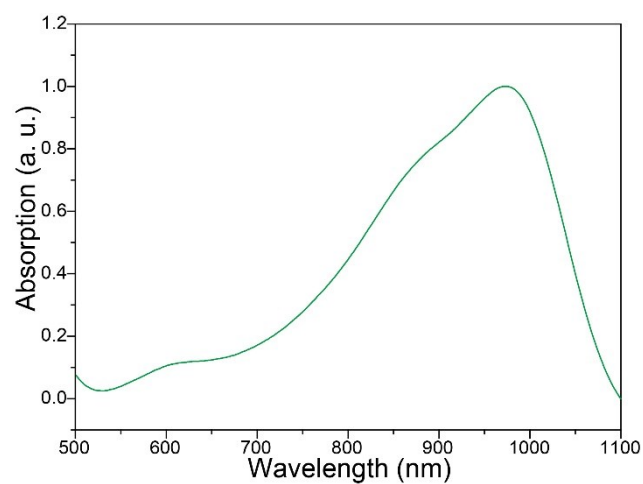**Figure S2**. Gel permeation chromatography (GPC) results of polymer BDT-TBZ.

Figure S3. Absorption spectra of BDT-TBZ polymer in THF solution.
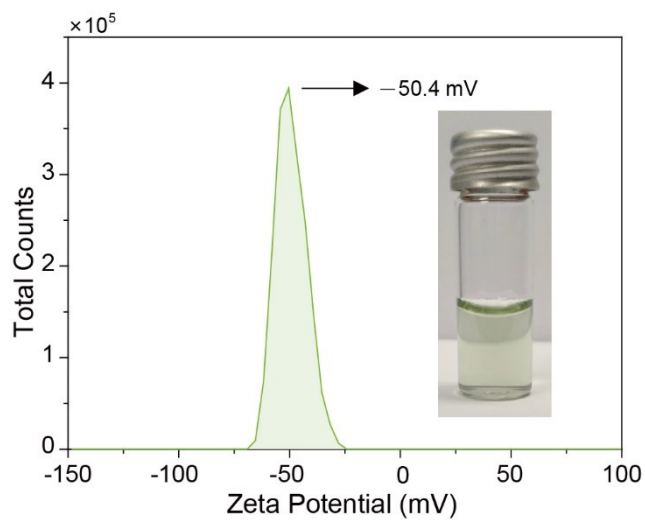

Figure S4. Zeta Potential of BDT-TBZ CPNs in water. Inset is a representative photo of BDT-TBZ suspension.
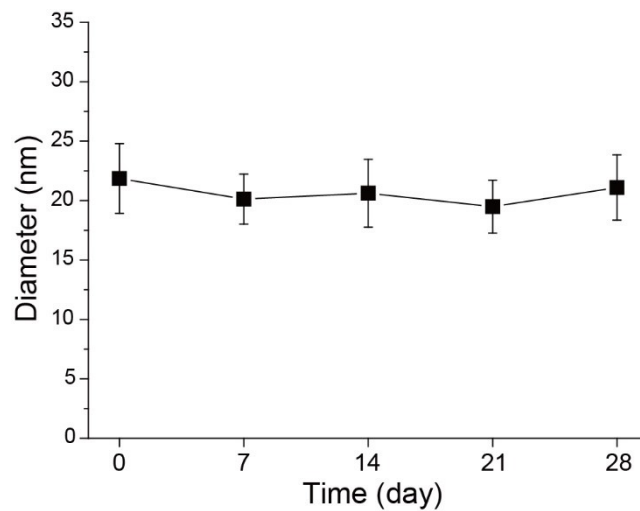
Figure S5. The hydrodynamic diameter changes of BDT-TBZ CPNs measured by DLS versus the storage time at 4 °C.
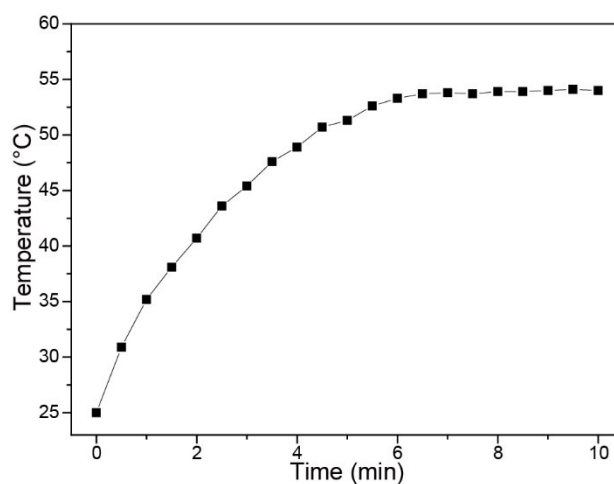

Figure S6. The temperature evolution of BDT-TBZ CPNs aqueous dispersion (100 μg mL^{-1}) under irradiation of 1064 nm laser (1 W cm^{-2}).
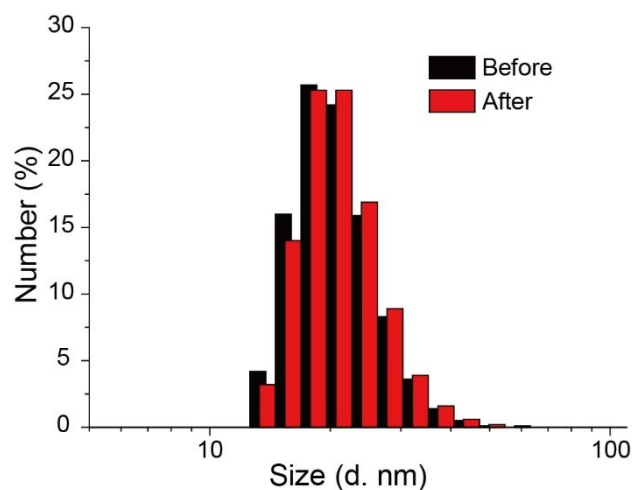
Figure S7. Size distribution of BDT-TBZ CPNs measure by DLS before and after five heating/cooling cycles (6 min for heating and 6 min for cooling as a cycle) under 1064 nm laser irradiation (1 W cm^{-2}).
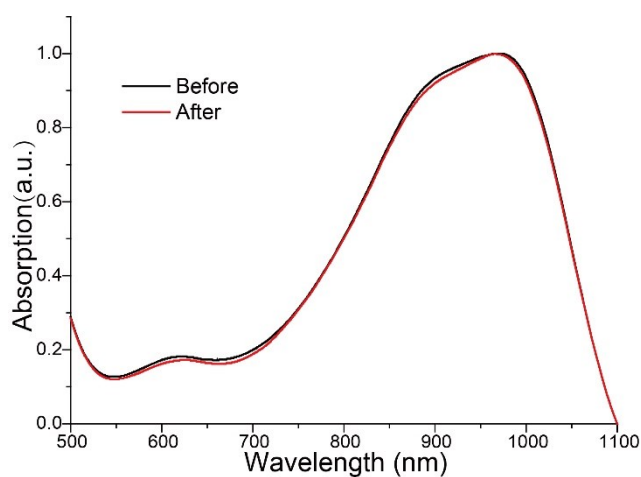

Figure S8. Absorption spectra of BDT-TBZ CPNs before and after five heating/cooling cycles (6 min for heating and 6 min for cooling as a cycle) under 1064 nm laser irradiation (1 W cm^{-2}).

Table S1. PCE and irradiation conditions of recently reported organic conjugated polymer nanoparticles (CPNs) and inorganic nanoparticles (IONPs) for photothermal therapy using 1064 nm laser.

| Type	Laser	PCE	Irradiation	Reference
OSPNs, CPNs	1064 nm	30.53 %	1.0 W cm^{-2}, 5 min	Biomaterials, 2020, 232, 119684
DPP-BTzTD L/S Pdots, CPNs	1064 nm	53 %	0.5 W cm^{-2}, 5 min	Adv. Funct. Mater., 2020, 30, 1909673
TBDOPV-DT NPs, CPNs	1064 nm	49.2 %	1.3W cm^{-2}, 10 min	Chem. Mater., 2017, 29, 718-725
SPN$_{I-II}$, CPNs	1064 nm	43.4 %	1.0 W cm^{-2}, 10 min	Adv. Mater., 2018, 30, 1705980
1T-MoS$_2$ nanodots, IoNPs	1064 nm	43.3 %	1.0 W cm^{-2}, 8 min	Small, 2020, 16, 2004173.
Sn$_x$ WO$_3$ tungsten bronze, IoNPs	1064 nm	18.6 %	2 W cm^{-2}, 10 min	Nanoscale, 2019, 11, 3300-3310
Cu$_2$MnS$_2$ NPs, IoNPs	1064 nm	49.38 %	0.6 W cm^{-2}, 10 min	Theranostics, 2017, 7, 4763–4776
Nb$_2$C NSs, IoNPs	1064 nm	27.03%	1.0 W cm^{-2}, 10 min	ACS Nano 2019, 13, 2223–2235
BDT-TBZ CPNs	1064 nm	55 %	1.0 W cm^{-2}, 6 min	This work
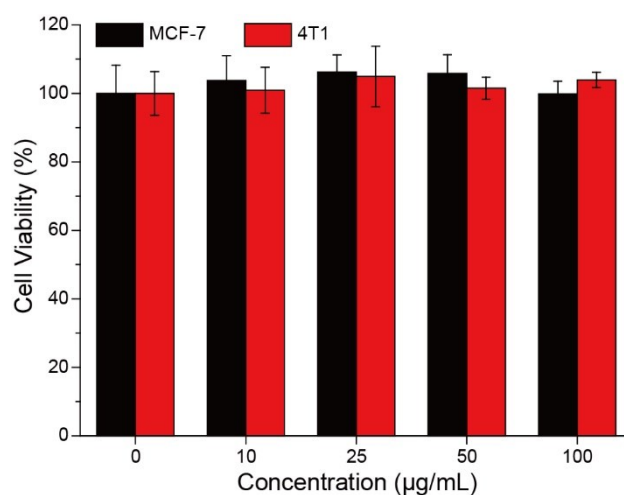
Figure S9. Relative cell viability of MCF-7 and 4T1 cells after incubation with different concentrations of BDT-TBZ CPNs for 24 h. Error bars indicate standard deviation (n = 6).
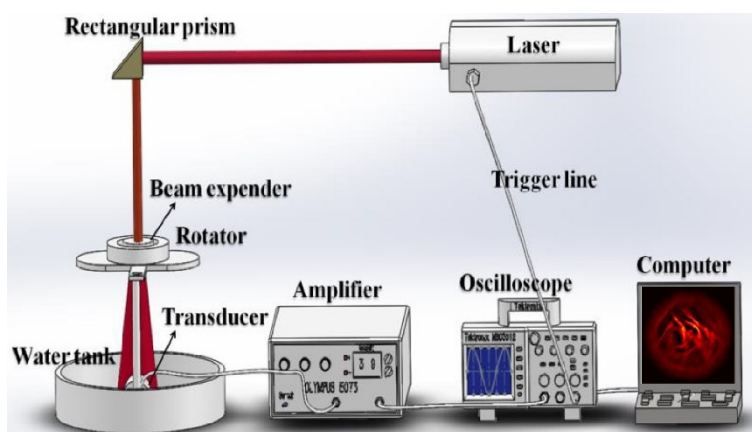

Figure S10. Schematic of the lab-built multispectral photoacoustic imaging system.

Table S2. Comparison of PA imaging results of BDT-TBZ and reported PA nanoagens

| Type	Injection	Laser	Maximum PA Signal Intensity	Reference
BDT-IID Pdots	intravenous injection	690 nm	~2.1-fold	ACS Appl. Mater. Interfaces, 2018, 10, 7012−7021
Pdots@hydrogel	intratumoral injection	808 nm	~1.7-fold	ACS Appl. Mater. Interfaces, 2020, 12, 51174−51184
DPP-DT-H Pdots	intratumoral injection	808 nm	~2.6-fold	Biomaterials, 2017, 144, 42-52
BDT-TBZ CPNs	intravenous injection	1064 nm	~2.7-fold	This work
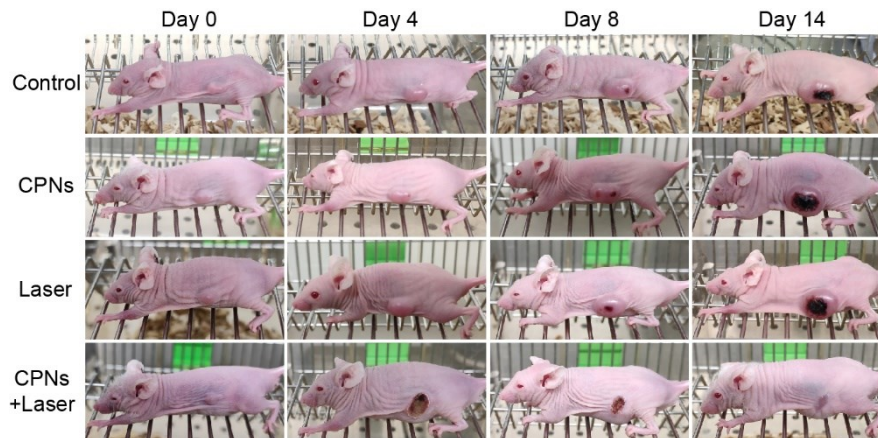
Figure S11. Representative 4T1 tumor-bearing mice photographs of four different groups after various treatments at different days. (i) Control; (ii) CPNs; (iii) Laser; (iv) CPNs, Laser (1064 nm, 1 W cm^{-2}, 6 min).
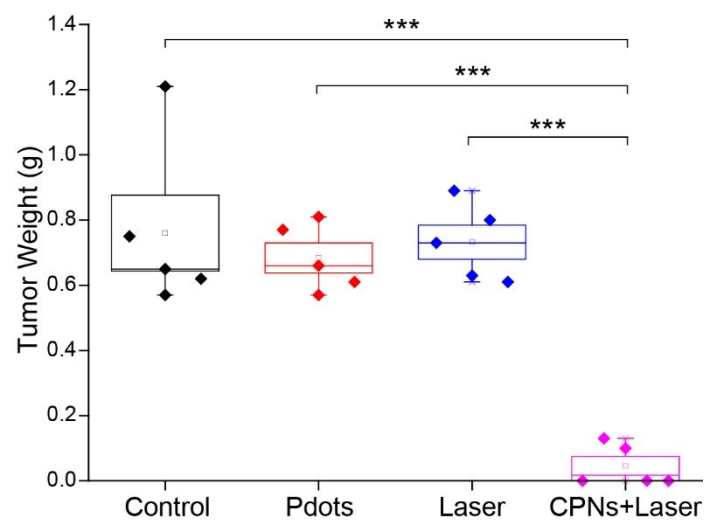
Figure S12. Tumor weight in various groups (*t* test unpaired analysis, ***$p < 0.001$).
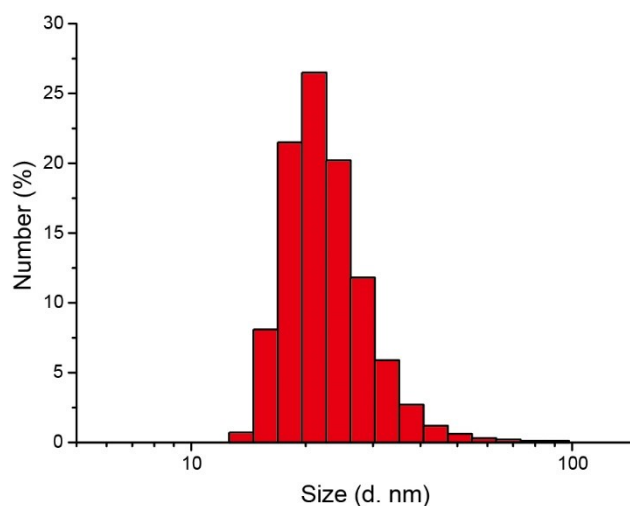

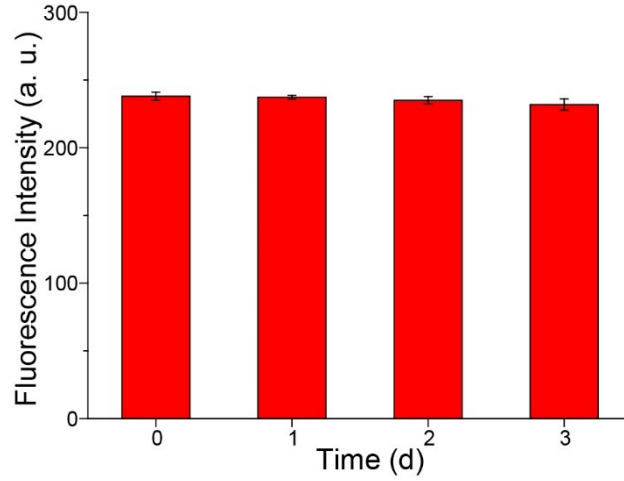**Figure S13**. The size distribution of NIR775-doped BDT-TBZ CPNs.

Figure S14. The relative fluorescence intensity of NIR 775-doped CPNs at different time intervals (0, 1, 2, and 3 d). Error bars indicate standard deviation (n=3).

3. Calculation: Photothermal Conversion Efficiency[1, 2]

The photothermal conversion efficiencies were calculated as follows. From an energy balance in a system, we can describe the total energy balance as:

$$\sum_i m_i C_{p,i} \frac{dT}{dt} = \sum_j Q_j = Q_I + Q_0 - Q_{ext}$$

(1)

Where the i terms $m_i C_{p,i}$ are products of mass and heat capacity of system components, T is aggregate system temperature, and t is time. The j energy terms Q_j include laser-induced energy source terms Q_I (from CPNs) and Q_0 (from solvent and container) as well as energy outputs Q_{ext}.

Q_I is the photothermal energy input from the CPNs, which can be described as:

$$Q_I = I(1 - 10^{-A_\lambda})\eta$$

(2)

Where I is incident laser power, η represents the efficiency of transducing incident resonant absorbance to thermal energy via plasmons, and A_λ is the absorbance at the used laser wavelength (1064 nm). Q_0 stands for the heat dissipated from light absorbed by the solvent and container, which can be measured independently using a container just containing aqueous samples without CPNs.

$Qexp$, external heat flux in the system, is nearly proportional to the linear thermal driving force, with a heat-transfer coefficient, h, as the proportionality constant.

$$Q_{ext} = hA(T - T_{amb})$$

(3)

Where h and A stand for heat transfer coefficient and surface area of the container, respectively. hA can be determined by measuring the rate of temperature decrease after removing the light source. In the absence of any laser excitation, $(Q_I + Q_0 = 0)$ substituting eq. (3) with eq. (1) gives

$$\sum_i m_i C_{p,i} \frac{dT}{dt} = -hA(T - T_{amb})$$

(4)

After rearrangement and integration, the following expression for t is obtained:

$$t = -(\frac{mC_p}{hA})In(\frac{T_{amb} - T}{T_{amb} - T_{max}})$$

(5)

Where m and C_p are the mass and heat capacity of water, respectively. In order to get the value of hA, a dimensionless driving force temperature, θ, is introduced, scaled using the maximum system temperature, T_{max}, and a sample system time constant τ_s.

$$\theta = \frac{T_{amb} - T}{T_{amb} - T_{max}}$$

(6)

$$\tau_s = \frac{mC_p}{hA}$$

(7)

Where τ_s is the slope of the linear time data from the cooling period.

$$t = -\tau_s \ln(\theta)$$

(8)

Then the photothermal conversion efficiency (η) can be calculated as:

$$\eta = \frac{hA(T_{max} - T_{amb}) - Q_0}{I(1 - 10^{-A_\lambda})}$$

(9)

References

1. D. K. Roper, W. Ahn and M. Hoepfner, *J. Phys. Chem. C*, 2007, **111**, 3636-3641.
2. H. B. Chen, J. Zhang, K. W. Chang, X. J. Men, X. F. Fang, L. B. Zhou, D. L. Li, D. Y. Gao, S. Y. Yin, X. J. Zhang, Z. Yuan and C. F. Wu, *Biomaterials*, 2017, **144**, 42-52.